applied sciences

MDPI

Article

XRF Semi-Quantitative Analysis and Multivariate Statistics for the Classification of Obsidian Flows in the Mediterranean Area

Letizia Bonizzoni *, Oleksandra Kulchytska and Giulia Ruschioni

Department of Physics "Aldo Pontremoli", University of Milan, Via Celoria 16, 20133 Milan, Italy
* Correspondence: letizia.bonizzoni@mi.infn.it

Abstract: Obsidian is a natural volcanic glass formed after eruptions if very rapid cooling of lava occurs. In particular conditions, the lava silicate ions cannot reach the crystalline lattice ordered formation and assume a chaotic arrangement, giving origin to obsidian flows. Obsidian has been used since the Paleolithic period to make tools because of its durability; in the Neolithic period, its trade played an important role in the Mediterranean area, and currently, obsidian is of particular interest for tracing prehistoric trading patterns. In this work, we present a semi-quantitative approach, exploiting energy-dispersive X-ray fluorescence (ED-XRF) coupled with principal component analysis. We consider geological samples from the five main collection sites of archaeological interest in the Mediterranean Basin (i.e., Pantelleria, Lipari, Palmarola, and Sardinia islands in Italy and Milos Island in Greece) and obtain a reliable classification of the fragments' provenance, also comparing chemical fingerprints with data from the literature. Reported results show that this non-invasive semi-quantitative protocol could ease the application to archaeological samples, such as blades and splinters, permitting the classification of artifacts found in the archeological sites of the Mediterranean area even when relatively few samples are considered.

Keywords: EDXRF; obsidian; semi-quantitative analysis; multivariate analysis; provenance classification

Citation: Bonizzoni, L.; Kulchytska, O.; Ruschioni, G. XRF Semi-Quantitative Analysis and Multivariate Statistics for the Classification of Obsidian Flows in the Mediterranean Area. *Appl. Sci.* **2023**, *13*, 3495. https://doi.org/10.3390/app13063495

Academic Editor: José A. González-Pérez

Received: 23 February 2023
Revised: 6 March 2023
Accepted: 7 March 2023
Published: 9 March 2023

1. Introduction

Obsidian is a volcanic glass, naturally occurring when lava extruded from an eruption cools rapidly with minimal crystal growth, and it is usually related to volcanic regions of young geological age. In particular conditions, the lava silicate ions cannot reach the ordered formation of a crystalline lattice and assume a chaotic arrangement, giving origin to obsidian flows. The sources of this material are few and well known, and obsidian artifacts, also due to their resistance to environmental deterioration, are considered some of the earliest evidence of commerce [1]. This is especially true for those periods which predate the manufacture of pottery, the material of choice for many archaeological studies due to its durability and diffusion. Actually, obsidian has been known since antique times, and it was already used at the end of the Paleolithic period to make knives and blades because of its durability. In the Neolithic period, its trade played an important role in the Mediterranean area: samples of polished obsidian have been found hundreds of kilometers from extraction sites, thus being of particular interest for tracing prehistoric trading patterns. Indeed, many published works about obsidian provenance refer to the Mediterranean basin [2–9], as this geographic area was the most important supplier in ancient times, even if sources were present also in the Carpathians, Anatolia, the Caucasus, and the Arabia peninsula.

Obsidian that was used for artifact production is usually chemically homogeneous both in its major and trace elements, and it is a good representative of the original source. Characterizing the sources thus allows to study the provenance of the artifacts. The primary constituents in obsidian are SiO_2 (up to 80%), Al_2O_3 (up to 15%), Na_2O, and K_2O (up to 5%) together with many minor and trace elements which largely vary from one source to another [10]. When dealing with a high number of geological obsidian samples, major and

trace element detection and quantification can even distinguish specific sub-sources [11,12], and this permits archaeological considerations about access to obsidian sources, territorial control, craft specialization, and mobility of populations.

Several chemical analyses have already proved their ability to distinguish sources of obsidian since the first studies in the 1960s [13–18]: the earliest measurements used emission spectrometry [19], atomic absorption spectrometry (AAS), flame photometry [20], and proton inelastic scattering [21]. Later, laser ablation–inductively coupled plasma mass spectrometry (La-ICP-MS), particle-induced X emission (PIXE) [4,22], and energy-dispersive spectroscopy with a scanning electron microscope (SEM-EDS) were applied [23] as well. One of the most used techniques is still neutron activation analysis (NAA) [2], a nuclear technique that has sometimes been coupled with particle-induced gamma emission (PIGE) [18] or X-ray fluorescence (XRF) [23]. This peculiar analytical technique guarantees high precision and a good range of elements detected, but it requires the irradiation of the samples with a neutron flux. Throughout the years, Raman micro-spectroscopy [22,24], Mossbauer spectroscopy [15], and optical emission spectroscopy (OES) [19] were also used for the same purpose.

Among the techniques applied for obsidian provenance studies, energy-dispersive X-ray fluorescence (ED-XRF) plays a leading role [5,25–32], as it in principle allows the performance of element quantification in a non-destructive manner with relatively low detection limits on samples of any size. Moreover, both portable and laboratory equipment are available for elemental quantification. Regardless, due to suboptimal detection ability for low Z elements, specific calculation and calibration software are required, resulting in the necessity of customizing data elaboration [10,33]. This obstacle is overcome, as the geographical origin discrimination based on XRF results is usually performed on the basis of element ratios rather than on the elemental concentration itself [2,23,27,31]; operating in this manner, reported results on obsidian samples clearly indicate the ability of this methodology to distinguish sample provenance either when obtained with tabletop XRF or portable XRF.

Multivariate statistics (MV) coupled to the determination of the chemical elements have been suggested [9] as a useful tool for a systematic approach to obsidian source characterization; they have been applied in a few cases, exploiting analytical results obtained from different techniques [34,35].

From these starting points, with the present work, we introduce a semiquantitative approach as a method of bypassing a lack of reliable quantification while still allowing the combined use of MV. This alternative protocol based on semi-quantitative XRF analysis and statistical data elaboration allows a clear separation between the various Mediterranean provenances of geological obsidian samples even if we have not considered sub-source discrimination yet.

2. Related Works

2.1. Quantitative ED-XRF Analysis of Obsidian Samples

When using ED-XRF for the quantitative analysis of glasses, ceramics, or low-Z matrix samples in general, the problem of evaluating self-absorption effects due to the non-detectable light element matrix (the so-called "dark matrix") arises [36]. In the specific case of obsidian, the light elements' presence can be quite different depending on the source, and this introduces a further element of complexity in calculations. In particular, medium–heavy elements' dispersion in light matrix can be detected and quantified under precise circumstances [37,38]. For instance, quantitative X-ray fluorescence analysis of vitreous materials can be obtained bypassing the problem of light-element matrix absorption evaluation by resorting to the concomitant measurement of incoherent Compton scattering intensity [36]. This method can be applied when dealing with "infinite thick" materials—that is, when the samples are thicker that the average X-ray penetration depth, which in turns depends on the chemical composition. An alternative method is to refer to the ratio between coherent Rayleigh and incoherent Compton scattering intensities, which

is, for instance, applied in "QXAS-AXIL" XRF spectra evaluation code [39]. In this latter case, non-infinite thickness samples can also be evaluated. During the evolution of this technique, there have been several studies dealing with the accuracy of non-destructive XRF measurements, especially on materials characterized by a light matrix. Some of these works refer to the determination of elements in obsidians [40] and require various separate excitation conditions together with several geochemical standards. Recent developments of this technique have made this option automated in some portable XRF spectrometers. Indeed, more recent research has shown that inter-instrumental calibration is needed when changing the ED-XRF device—for example, when using different portable XRF spectrometers [41]. This is still due to the difference between the non-detectable matrix for obsidian from different provenances.

2.2. Obsidian Sources Discrimination by ED-XRF

In general, rocks of the same type but different geographic provenance can be distinguished by means of elemental analyses as they contain typical trace elements [42]; actually, obsidian from different sources has distinct concentration patterns for the different elements. Available literature about source discrimination refers to some elements as markers of different origins, and different elements are considered depending on the aim. Referring only to the sources considered in the present work, Sr and Zr were used for the identification of the provenance of Corsican obsidian finds [32], while Rb, Nb, Zr, and rare earth contents allowed the identification of Palmarola obsidian [12]. Fe, Sr, Rb, and their ratios were the markers for Lipari sub-sources [27,28,31], while Rb and Zr can be used to discriminate sub-sources in Pantelleria [26]. Again, Rb/Nb and Sr/Nb ratios obtained via non-destructive portable XRF are able to distinguish Monte Arci (Sardinia) sub-sources, as well as Lipari and Pantelleria sub-sources [30]. Monte Arci sub-sources can also be discriminated using K_2O/CaO ratio [29]. Our aim is instead to use as many elements as possible to obtain a discrimination without sorting out proper elements but instead exploiting MV potential. It is worth noting that the variability of single elements withing the same source is quite high due to the presence of sub-sources; for this reason, average data available in the literature sometimes have large relative errors.

3. Materials and Methods

3.1. Obsidian Geological Samples

In the present work, 33 geological samples from the five main sources in the Mediterranean basin were considered, as indicated in Figure 1. Most of the samples are from the Italian islands, namely 10 from Pantelleria (PNT1-PNT10), 4 from Palmarola (PA1-PA4), 4 from Sardinia-Monte Arci (MN1-MN4), and 12 from Lipari (LP1-LP12). Four more samples are from the Aegean Sea, namely from Milos Island in Greece (PM1-PM4). Ongoing studies are enlarging this data set, which will later be used as a reference for the classification of archaeological samples. In fact, from the archaeological point of view, the Mediterranean islands of Lipari, Melos, Palmarola, Pantelleria, and Sardinia have always been known as obsidian sources, and the raw material from these different sources can be clearly distinguished as they show different chemical–physical characteristics [12]. For instance, Monte Arci obsidian is grayish and shiny and very rich in microlites and phenocryst, while Pantelleria samples are poor in microlites, gray-greenish in color and relatively transparent. Both Lipari and Palmarola have a vitreous aspect, the former black and shiny and the latter black and semi-opaque [4].

The samples considered in the present work have been supplied during the last decades to the Laboratory for Fission Track Dating (FTD) of the University of Milan and underwent FTD age determination. Indeed, a possible alternative to the chemical characterization for discriminating obsidian sources and provenance is the fission track dating method, a radiometric technique [43]. In fact, the comparison of fission track parameters, such as age and track densities, has already been used as a different tool for correlating obsidian artifacts with their potential natural sources. This method was

applied by various research groups in the field of fission track dating considering various regions [44–46], and outcomes can be matched to those obtained via chemical composition characterization, especially when the chemical fingerprint does not fully discriminate different sources.

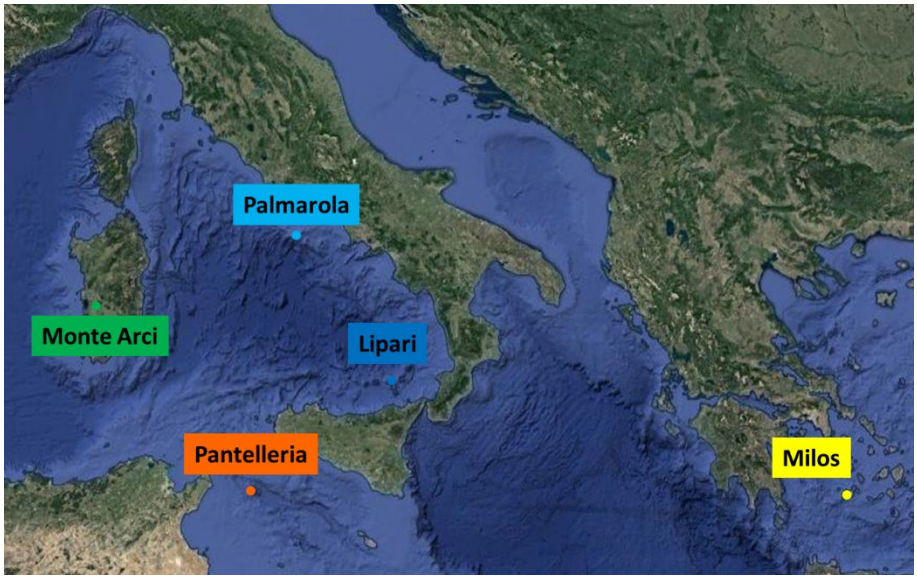

Figure 1. Geographical location of considered obsidian sources in the Mediterranean basin.

Please note that for this first study, we did not consider further information about sample sub-sources as it is not in the aim of the present work and as the number of samples considered is relatively small. It is worth also noting that materials from geological sources should not require a non-invasive protocol, but on the other hand, the final scope of this characterization is the future classification of archaeological samples, such as splinters and blades, clearly more prone to a non-destructive approach.

3.2. X-ray Fluorescence Analysis

Energy-dispersive X-ray fluorescence (EDXRF) analysis was performed on thick samples using the FUXYA2020 spectrometer [47], a homemade portable EDXRF spectrometer equipped with a MINI-X2 X-ray tube (Amptek, Bedford, MA, USA) with a maximum power of 4 W (50 kV, 0.2 mA) and a transmission rhodium anode. The X-ray detector used is XGL-SPCM-DANTE25, a complete SDD spectrometer from XGLAB Bruker Nano Analytics Division (Milan, Italy) with 17 mm^2 active area, 500 µm thickness, and 12.5 µm Be window. FUXYA2020 has a typical 45°–45° geometric configuration: the angle between the X-ray tube and the detector is set at 90° [47]. No filters were mounted on the exit window of the X-ray tube, so we used unfiltered continuous radiation emitted from the device: the continuous energy distribution allowed to have a better excitation for low Z elements. Regardless, energies below 2 keV were poorly detected, as detector efficiency is limited in this region due to the thickness of its entrance Be window. For instance, Si K lines (1.7 and 1.8 keV for Kα and Kβ, respectively) were detected, but the evaluation of their area was affected by a relatively high error due to the background to peak ratio; for this reason, elements under K (3.3 keV for Kα line) were not considered for MV elaboration. The radiation produced by the X-ray tube was collimated by a 2 mm diameter pinhole; the irradiated surface on the sample was therefore about 30 mm^2, so as to investigate a representative area of each sample. Thick obsidian blocks were measured without any preparation on flat surface areas. More than one point was considered on each of the 33 fragments under investigation to achieve a better statistic.

The working conditions were 40 kV and 0.6 mA with a 300 s acquisition time. Spectra deconvolution and area calculation were performed using the AXIL-QXAS 3.6 (Quantitative

X-ray Analysis System) software developed by IAEA, subtracting the background signals for each considered peak; in this way, a good discrimination between K and L series can be also be performed in case of very close energy values. Sixteen elements were detected and considered, namely K, Ca, Ti, Mn, Fe, Cu, Zn, Rb, Sr, Y, Zr, Nb, La, Ce, Pb, and Th; their areas were normalized to the Rayleigh scattering peak of rhodium (20.2 keV for Kα line) to eliminate eventual differences deriving from geometrical issues. Indeed, even when considering trace elements, the probability that obsidian from two different sources will have the same concentration of a few given elements within the experimental errors must not be overlooked. To reduce the probability of coincidental similarity it is useful to consider as many elements as possible, and MV analysis is the best way to handle such a huge amount of data. Multivariate analyses were performed considering semi-quantitative data [48] without calculating concentration values for the detected chemical elements. This approach already proved to be useful for glass classification on the bases of chromophore elements detected by XRF [49].

3.3. Multivariate Analyses

To give a graphic representation of the data and a more precise evaluation of the similarity between the samples, we performed both principal component analysis (PCA) and hierarchical cluster analysis (HC). Indeed, PCA and HC are the most widely used tools for exploring similarities and hidden patterns among samples and are used mostly when relationship on data and grouping are unclear. Both PCA and HC do not require any information about class membership or other response variables to obtain the graphical representation (unsupervised methods). This aspect makes the two methods suitable for the so-called exploratory data analysis [50]. PCA creates a low-dimensional representation of the samples from a data set, containing as much of the variance in the original data set as is possible. Moreover, it provides a representation of the variables that is directly connected to that of the samples and allows the user to visually find variables that are characteristic of specific sample groups. On the other hand, HC builds a dendrogram (i.e., a tree diagram) where the leaves are the individual objects (samples or variables, depending on the aim). Hierarchical clustering will always calculate clusters, even if there is no strong signal in the data; quite the opposite, in the same situation PCA will present a plot similar to a cloud with samples evenly distributed.

PCA was performed, exploiting the prcomp function of the R stats package [51], and the calculation was made by means of singular value decomposition on the data matrix. Before performing the analysis, the variables were scaled to have a unit variance, and then the correlation matrix was calculated. The 2D plot was obtained by means of pca3d package (version 0.10.2). For HC, we previously auto-scaled the semi-quantitative data as areas for detected chemical elements can highly differs in values, and we used the software Minitab 18®.

4. Results and Discussion

4.1. Direct Comparison of Spectra and Semi-Quantitative Results

The first step through the validation of our methodology is a qualitative evaluation to check if any inconsistency with literature data (see Section 2.2) is present. Differences between geological provenances for our samples were thus at first studied from the qualitative comparison of XRF spectra; this procedure allows the identification of sixteen elements on which to base chemometric elaboration. As reported in Section 2, the chosen elements are K, Ca, Ti, Mn, Fe, Cu, Zn, Rb, Sr, Y, Zr, Nb, La, Ce, Pb, and Th. A few elements with energy emissions lower that K, such as Si, were also detected; regardless, the evaluation of their peak areas was affected by a relatively high error, and they were considered not suitable for MV elaboration as they could have added some statistical noise. Figure 2 reports one typical spectrum for each provenance using the same color code as in Figure 1. Spectra obviously appear to be normalized to the Rayleigh diffusion peak (Rh R in Figure 2) without any data elaboration as all spectra have been acquired in the same irradiating and

geometrical conditions. Only more evident elements have been indicated in the spectra reported in Figure 2; please note that the Fe Kα peak in Pantelleria spectrum is cut due to the vertical scale to allow the comparison of less-present elements from the various provenance. Differences were then investigated using direct comparison and bivariate analyses to check correspondence with literature data: for each detected element, peak area of the principal line of the K or L series was evaluated by spectra fitting using the AXIL-QXAS 3.6 software developed by IAEA considering the background and the possible superimposition between different elements. Semi-quantitative values [52] were obtained considering the intensity of emission in cps (count per second) for each element normalized to the relative sensitivity for the specific element [48]; in the following, we will refer to the semi-quantitative values obtained as to "relative concentration" for the sake of brevity.

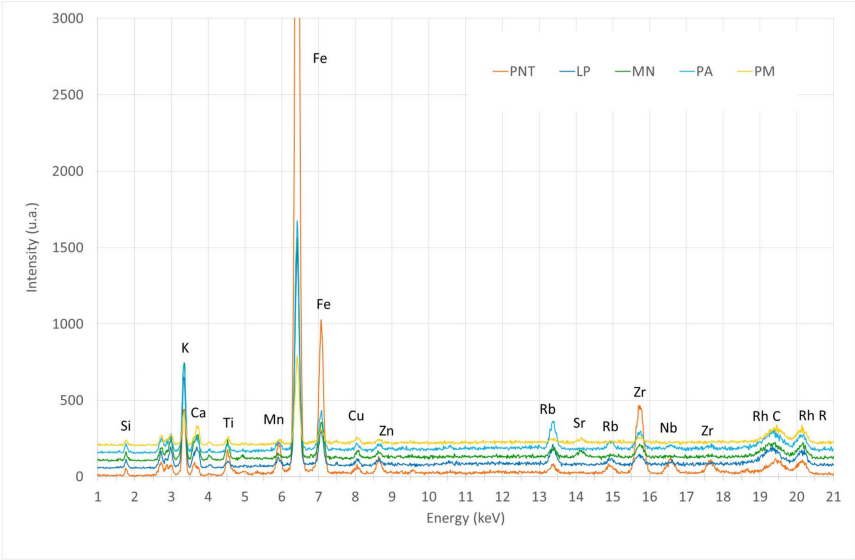

Figure 2. Comparison between representative XRF spectra for the five obsidian sources considered in the present paper: Pantelleria (PNT), Palmarola (PA), Sardinia-Monte Arci (MN), Lipari (LP), and Milos Island (PM). Only the main elements are reported. Spectra are normalized to the Rayleigh diffusion peak due to the acquisition conditions; Pantelleria spectrum has been cut in the vertical axis.

From comparison between the XRF spectra obtained for considered geological regions and literature data, it is clear that Pantelleria is the easiest to recognize; indeed, Pantelleria obsidian shows much higher Fe, Zr, and Mn contents, as evident from the bar chart reported in Figure 3.

Considering the average semi-quantitative values obtained for Fe in the different groups (named in Figure 3 and in the following as PNTav, PAav, MNav, PMav, and LPav), we can calculate a content 3 to 4 times higher in Pantelleria samples [28]. The same applies to other elements, such as Ti, Nb, and Zn. These details about minor elements are coherent with literature data, even though high relative errors are present within the same provenance, depending also on the exploited technique [27,31], as stressed in Section 2.2.

In the Pantelleria sample spectra, we also detected some elements that are under the minimum detection limit of our spectrometer [16] in the obsidian samples from the other considered sources. This is the case of La and Ce [5,28]. It is worth noting that the detection of these elements is performed on the L series (4.6 and 5, and 4.8 and 5.3 keV respectively), which partially was superimposed to the K series of Ti (4.5 and 4.9 keV). The identification has been based on the Kα/Kβ and Lα/Lβ ratios via AXIL deconvolution subroutine, but the quantification of peak areas can be subject to larger errors. Regardless, La and Ce were not considered when performing statistical elaborations as they have been detected only in Pantelleria obsidians.

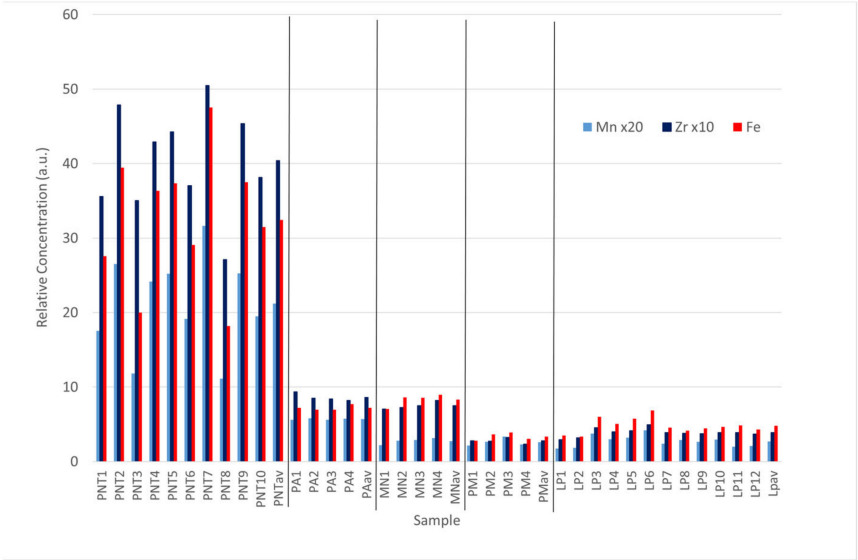

Figure 3. Relative concentration of Mn, Zr, and Fe; for each class, the average value of the reported elements is also shown (PNTav, PAav, MNav, PMav, LPav). Samples' codes are the following: Pantelleria (PNT), Palmarola (PA), Sardinia-Monte Arci (MN), Lipari (LP), Milos Island (PM).

Bivariate graphs (not reported in this paper) obtained from our data allowed us to discriminate one or two sources from the others depending on the chosen elements or element ratios, but we were not able to discriminate all the classes at once. As a few examples, the plot of the relative concentration of Rb vs. Nb allowed us to discriminate Palmarola and Pamtelleria materials from the three other sources. Pantelleria was again recognized by plotting the ratios of Rb/Nb vs. Sr/Nb, but Monte Arci and Porto Melos were grouped together, such as Palmarola and Lipari materials. The best results applying bivariate analysis to discriminate the five considered provenance were obtained plotting Sr/Fe vs. Rb/Fe, but again, Porto Melos and Monte Arci samples are not distinguishable yet.

4.2. Multivariate Analyses on Semi-Quantitative Data

As already stated, we choose to apply a MV approach so to consider as many variables as useful for a reliable discrimination. Indeed, appropriate statistical methods can be used to handle all the variables at a time on possibly large sample sets when dealing with a relatively high number of variables—for instance, chemical elements. These methods have already proved to work on concentration data [53], but also on semiquantitative data or on XRF spectra [48,49]. Actually, they also permit the consideration of analytical results from different techniques in one unique elaboration to classify samples [42]. The fourteen selected elements detected in all the samples (namely: K, Ca, Ti, Mn, Fe, Cu, Zn, Rb, Sr, Y, Zr, Nb, Pb, and Th) were considered for MV elaborations; statistical elaboration was applied to all the measured samples with the addition of the five average virtual samples obtained, one for each class—namely, PNTav, PAav, MNav, PMav, and LPav—as defined above through the relative concentration average values.

In Figure 4, the result of HC elaboration for our obsidian samples is reported; original data have been auto-scaled, and average linking method coupled with Euclidean distance has been used. The scaling of data is mandatory as different chemical element peak areas can have different orders of magnitude. The five groups for the five provenances are easily identified and are highlighted in the dendrogram with the same color code as Figure 1. Comparable results have been obtained by applying PCA to the same set of samples and detected elements, as evident by the scatter plot reported in Figure 5, in which larger dots represent the group centroids, while small dots represent the samples; explained variance for the first three PCs was about 88%. The groups are indeed quite well separated already by the score plot of the two first PCs, explaining a variance of about 69% (see Figure 5).

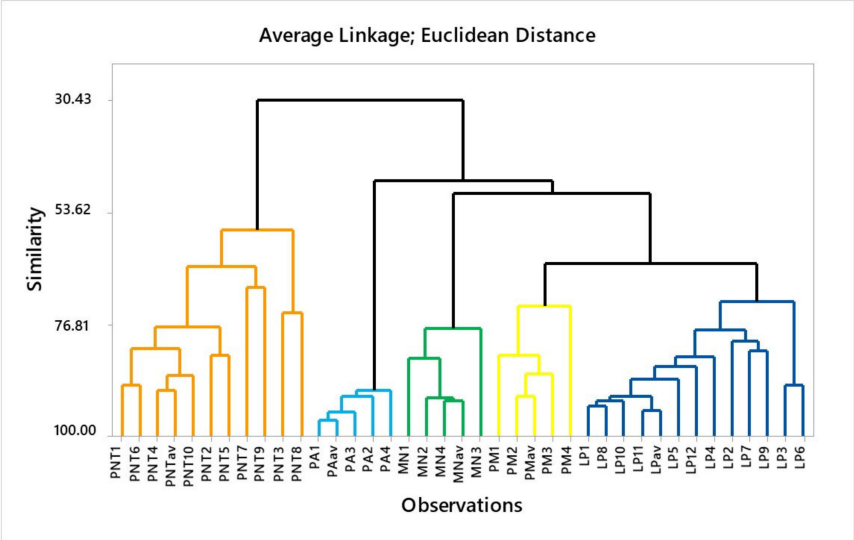

Figure 4. Dendrogram obtained for obsidian samples—Pantelleria (PNT), Palmarola (PA), Sardinia-Monte Arci (MN), Lipari (LP), Milos Island (PM)—considering all the elements; data have been auto-scaled, and average linking method coupled with Euclidean distance has been used. Colors are the same as in Figure 1.

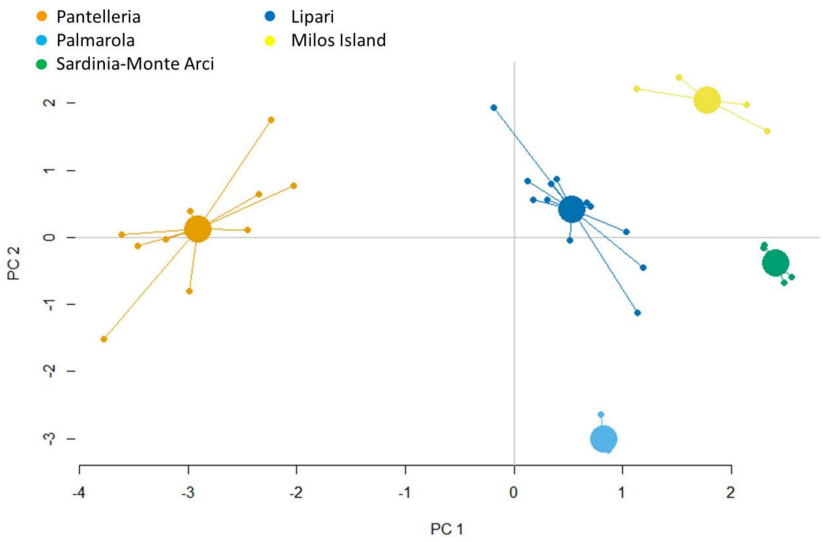

Figure 5. Score plot obtained considering the complete dataset used for dendrogram reported in Figure 3. The variance accounted by the first two PC is about 69%. Colors are the same as in Figure 1; samples' names are not reported for sake of clarity.

From the relative loading plot (not reported), correlation between the original variables and their loading were highlighted, allowing us to select the most significant variables and to increase variance up to 92% for the first three PCs. This result was obtained using a set of data (Data Set I) composed of some of the variables (namely, Fe, Cu, Rb, Sr, Zr, Y, Th) for all the samples. Score and loading plots for the first two PCs are reported in Figures 6 and 7, respectively; larger dots in the scatter plot represent the group centroids, while small dots represent the samples. For PC1 and PC2 alone, the explained variance is 76%, but the different groups are already evident. It is interesting to note that the dendrogram (not reported) obtained with the same parameters as that reported in Figure 4 (average linkage, Euclidean distance) for Data Set I is not as reliable as the one obtained on the complete dataset, as a few samples (namely PM4 and MN3) are misclassified in the wrong groups.

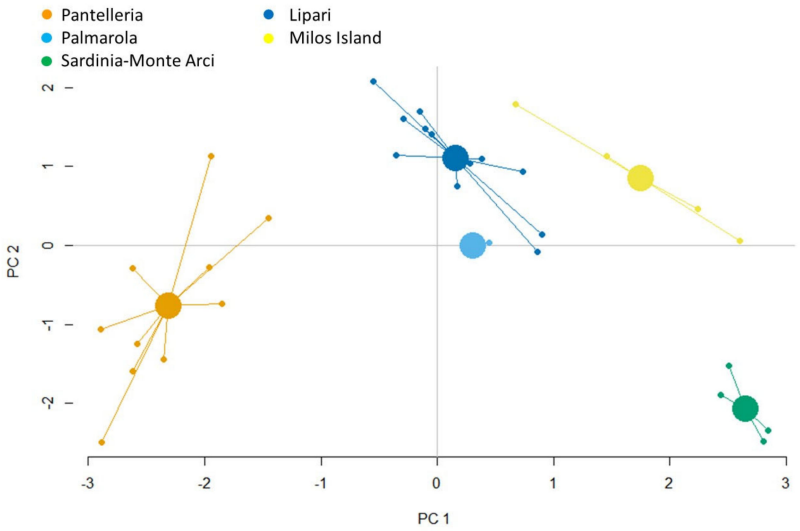

Figure 6. Score plot obtained considering Data Set I. The variance accounted by the first two PC is 76%. Colors are the same as in Figure 1; samples' names are not reported for sake of clarity.

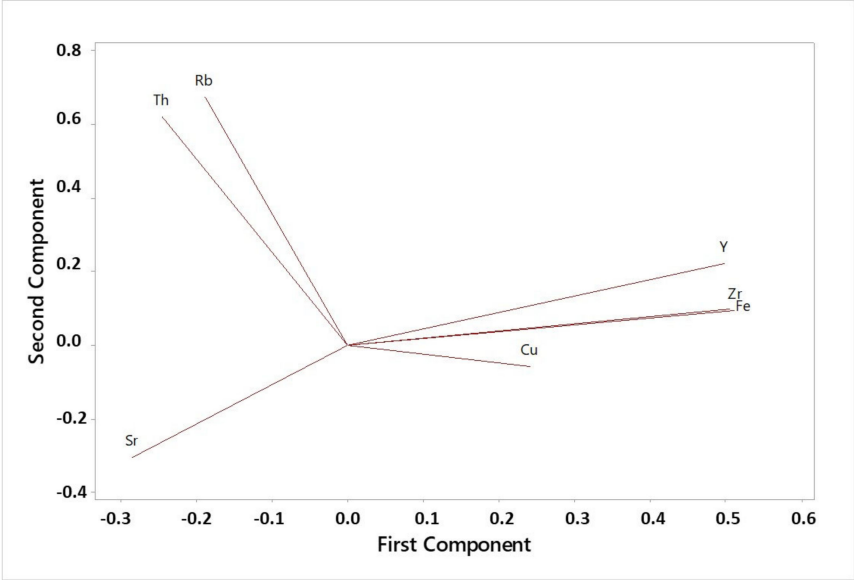

Figure 7. Loading plot obtained considering Data Set I. The variance accounted by the first two PC is 76%.

We also considered a second set of variables (Data Set II) to undergo MV, selecting those elements used for bivariate graphs in the quoted papers, and namely K, Ca, Fe, Cu, Rb, Sr, and Zr. In this case, we obtained a variance of about 87% for the first three PCs, lower than the one calculated both for the complete dataset and for Data Set I. Score plot and loading plot for Data Set II are reported in Figures 8 and 9, respectively; larger dots in the scatter plot represent the group centroids, while small dots represent the samples. For PC1 and PC2 alone, the explained variance is about 78%, but the different groups are already evident and more compact that those obtained for Data Set I even if they explain a lower variance. Similarly to what happened considering Data Set I, the dendrogram obtained for Data Set II (not reported) misclassified some samples, and it is not as useful a reference as the diagram obtained considering all the detected elements. More in detail, using the elements selected for Data Set II—i.e., those considered in the quoted papers for bivariate graph—to distinguish subgroups led to the clear discrimination of only Pantelleria samples, while the other groups are more confused.

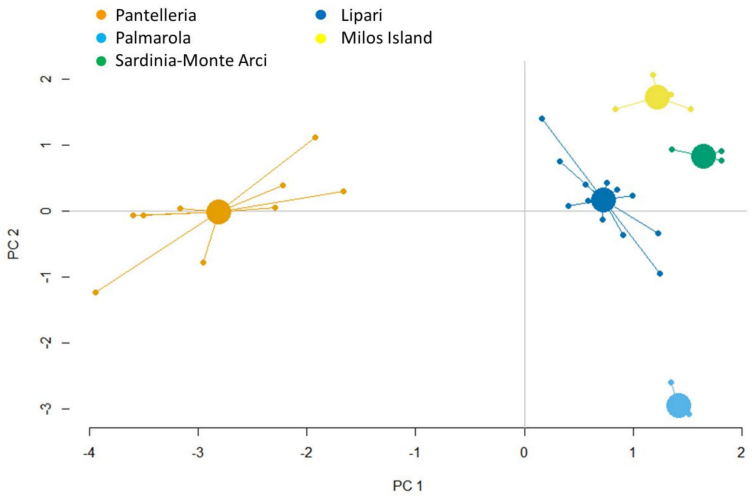

Figure 8. Scatter plot obtained considering Data Set II. The variance accounted by the first two PC is about 68%. Colors are the same as in Figure 1; samples' names are not reported for sake of clarity.

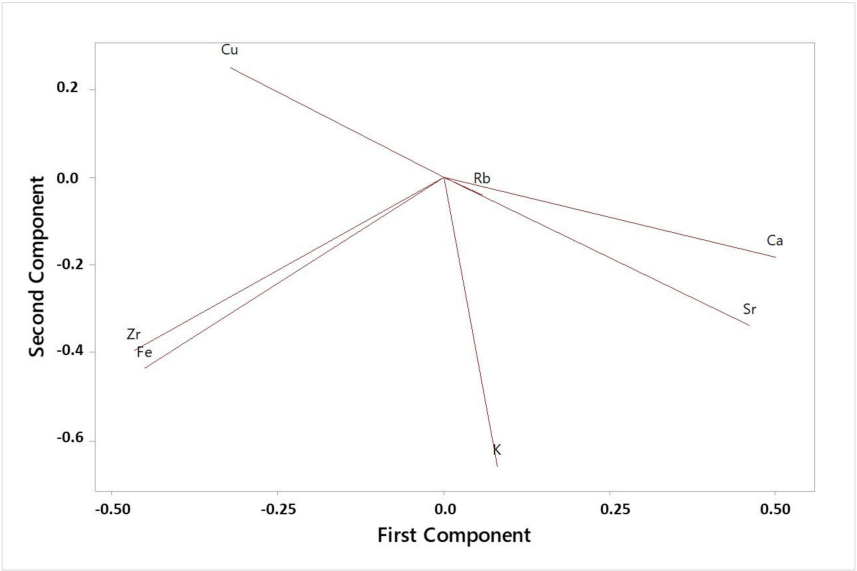

Figure 9. Loading plot obtained considering Data Set II. The variance accounted by the first two PC is about 68%.

Indeed, the more elements we consider, the better result we achieve through HC analysis. It is worth stressing once again that lower-Z elements, such as Si, were not considered for MV data elaboration even if detected so as to not introduce statistical noise, as the quantification of their peak areas was affected by a large error due to the low detector efficiency for low energies.

5. Conclusions and Future Perspectives

The Mediterranean Basin was the most important supplier of obsidian in ancient times. In particular, the Mediterranean islands of Lipari, Melos, Palmarola, Pantelleria, and Sardinia. This natural glass has been used since the Palaeolithic period to make tools because of its durability; its trade during the Neolithic period played an important role and individuating the source of artifact material is of particular interest to trace prehistorical trading patterns. The present paper presents a non-invasive protocol for obsidian flow discrimination based on semi-quantitative determination of chemical elements by portable XRF. Indeed, for the considered geological samples, results allowed to differentiate the

sources in the Mediterranean basin when considered together thank to powerful of MV data elaboration and without any other information about provenance. Indeed, the more elements we consider, the better result we achieve through HC analysis.

The applied protocol is valid even if a relatively low number of samples has been considered and allows to bypass the critical step of obtaining a reliable quantitative analysis by XRF spectra on raw obsidian fragments.

For the future, we intend to extend this approach to the classification of archaeological samples on the bases of the groups obtained in this preliminary study. Moreover, considering a higher number of geological samples, we intend to apply the same procedure for the discrimination of sub-sources and, as a consequence, to classify archaeological samples in relation to the specific exploited lava flow. The method presented in this paper, based on the semiquantitative analyses of minor and trace elements by XRF, could benefit from the comparison of results obtained via fission track dating analysis.

Another innovative complementary technique now under investigation is the application of the study of radioactive isotope ratios, that is to study a method that uses natural radioactive isotopes as markers. This approach goes in the same direction of the one proposed in the present paper and can provide a number of advantages, such as avoiding the need for calibration or the destruction of the samples, which is extremely important in the case of obsidian archaeological objects from museums or other collections. This methodological approach will benefit from the use of chemometric analyses as well.

Author Contributions: Conceptualization, L.B. and O.K.; methodology, L.B.; investigation, O.K.; data analyses: L.B., O.K. and G.R.; writing—original draft preparation, L.B.; writing—review and editing, L.B. and G.R.; supervision, L.B. All authors have read and agreed to the published version of the manuscript.

Funding: This research received no external funding.

Institutional Review Board Statement: Not applicable.

Informed Consent Statement: Not applicable.

Data Availability Statement: Data are available on request to the corresponding author.

Acknowledgments: The authors are grateful to Alessandra Guglielmetti (Department of Physics "Aldo Pontremoli", University of Milan) for providing the obsidian samples studied in this work.

Conflicts of Interest: The authors declare no conflict of interest.

References

1. Bonizzoni, L.; Martinelli, M.C.; Coltelli, M.; Manni, M.; Balestrieri, M.L.; Oddone, M.; Guglielmetti, A. New Perspectives on an "Old" Technique: Lipari Obsidian and Neolithic Communities Investigated by Fission Track Dating. *J. Phys. Conf. Ser.* **2022**, *2204*, 012032. [CrossRef]
2. Avino, P.; Rosada, A. Mediterranean and Near East Obsidian Reference Samples to Establish Artefacts Provenance. *Herit. Sci.* **2014**, *2*, 16. [CrossRef]
3. Rotolo, S.G.; Carapezza, M.L.; Correale, A.; Martin, F.F.; Hahn, G.; Hodgetts, A.G.E.; Monica, M.L.; Nazzari, M.; Romano, P.; Sagnotti, L.; et al. Obsidians of Pantelleria (Strait of Sicily): A Petrographic, Geochemical and Magnetic Study of Known and New Geological Sources. *Open Archaeol.* **2020**, *6*, 434–453. [CrossRef]
4. Acquafredda, P.; Andriani, T.; Lorenzoni, S.; Zanettin, E. Chemical Characterization of Obsidians from Different Mediterranean Sources by Non-Destructive SEM-EDS Analytical Method. *J. Archaeol. Sci.* **1999**, *26*, 315–325. [CrossRef]
5. Acquafredda, P.; Micheletti, F.; Muntoni, I.M.; Pallara, M.; Tykot, R.H. Petroarchaeometric Data on Antiparos Obsidian (Greece) for Provenance Study by SEM-EDS and XRF. *Open Archaeol.* **2019**, *5*, 18–30. [CrossRef]
6. Muntoni, I.M.; Micheletti, F.; Mongelli, N.; Pallara, M.; Acquafredda, P. First Evidence in Italian Mainland of Pantelleria Obsidian: Highlights from WD-XRF and SEM-EDS Characterization of Neolithic Artefacts from Galliano Necropolis (Taranto, Southern Italy). *J. Archaeol. Sci. Rep.* **2022**, *45*, 103553. [CrossRef]
7. Francaviglia, V. Characterization of Mediterranean Obsidian Sources by Classical Petrochemical Methods. *Charact. Mediterr. Obsidian Sour. Class. Petrochem. Methods* **1984**, *20*, 311–332.
8. Glascock, M.D.; Braswell, G.E.; Cobean, R.H. A Systematic Approach to Obsidian Source Characterization. In *Archaeological Obsidian Studies: Method and Theory*; Shackley, M.S., Ed.; Advances in Archaeological and Museum Science; Springer: Boston, MA, USA, 1998; pp. 15–65, ISBN 978-1-4757-9276-8.

9. Glascock, M.D. A Systematic Approach To Geochemical Sourcing Of Obsidian Artifacts. *Sci. Cult* **2020**, *2*, 35–47. [CrossRef]
10. Giauque, R.D.; Asaro, F.; Stross, F.H.; Hester, T.R. High-Precision Non-Destructive X-ray Fluorescence Method Applicable to Establishing the Provenance of Obsidian Artifacts. *X-ray Spectrom.* **1993**, *22*, 44–53. [CrossRef]
11. Tykot, R.H. Obsidian Studies in the Prehistoric Central Mediterranean: After 50 Years, What Have We Learned and What Still Needs to Be Done? *Open Archaeol.* **2017**, *3*, 264–278. [CrossRef]
12. Macchia, A.; Malorgio, M.; Plattner, S.H.; Tiepolo, M.; Ferretti, M.; Ferro, D.; Campanella, L.; Zarattini, A. The Obsidian Palmarola: Markers of Origin–A Example of Exploratory Data Analysis. In Proceedings of the CMA4CH, Mediterranean Meeting, Application of Multivariate Analysis to Cultural Heritage and Environment 3rd edition, Taorimina, Italy, 26–29 September 2010.
13. Summerhayes, G.R. Obsidian Network Patterns In Melanesia–Sources, Characterisation and Distribution. *Bull. Indo-Pac. Prehistory Assoc.* **2009**, *29*, 109–123. [CrossRef]
14. Torrence, R.; Neall, V.; Doelman, T.; Rhodes, E.; McKee, C.; Davies, H.; Bonetti, R.; Guglielmetti, A.; Manzoni, A.; Oddone, M.; et al. Pleistocene Colonisation of the Bismarck Archipelago: New Evidence from West New Britain. *Archaeol. Ocean.* **2004**, *39*, 101–130. [CrossRef]
15. Stewart, S.J.; Cernicchiaro, G.; Scorzelli, R.B.; Poupeau, G.; Acquafredda, P.; De Francesco, A. Magnetic Properties and 57Fe Mössbauer Spectroscopy of Mediterranean Prehistoric Obsidians for Provenance Studies. *J. Non-Cryst. Solids* **2003**, *323*, 188–192. [CrossRef]
16. Blackman, M.J. Provenance Studies of Middle Eastern Obsidian from Sites in Highland Iran. In *Archaeological Chemistry—III*; Advances in Chemistry; American Chemical Society: Washington, DC, USA, 1984; Volume 205, pp. 19–50. ISBN 978-0-8412-0767-7.
17. Golitko, M.; Meierhoff, J.; Terrell, J.E. Chemical Characterization of Sources of Obsidian from the Sepik Coast (PNG). *Archaeol. Ocean.* **2010**, *45*, 120–129. [CrossRef]
18. Gratuze, B.; Barrandon, J.N.; Isa, K.A.; Cauvin, M.C. Non-Destructive Analysis of Obsidian Artefacts Using Nuclear Techniques: Investigation of Provenance of Near Eastern Artefacts. *Archaeometry* **1993**, *35*, 11–21. [CrossRef]
19. Cann, J.R.; Renfrew, C. The Characterization of Obsidian and Its Application to the Mediterranean Region. *Proc. Prehist. Soc.* **1964**, *30*, 111–133. [CrossRef]
20. Armitage, G.C.; Reeves, R.D.; Bellwood, P. Source Identification of Archaeological Obsidians in New Zealand. *N. Z. J. Sci.* **1972**, *15*, 408–420.
21. Coote, G.E.; Whitehead, N.E.; McCallum, G.J. A Rapid Method of Obsidian Characterisation by Inelastic Scattering of Protons. *J. Radioanal. Chem.* **1972**, *12*, 491–496. [CrossRef]
22. Bellot-Gurlet, L.; Dorighel, O.; Poupeau, G. Obsidian Provenance Studies in Colombia and Ecuador: Obsidian Sources Revisited. *J. Archaeol. Sci.* **2008**, *35*, 272–289. [CrossRef]
23. Tykot, R.H. Chemical Fingerprinting and Source Tracing of Obsidian: The Central Mediterranean Trade in Black Gold. *Acc. Chem. Res.* **2002**, *35*, 618–627. [CrossRef]
24. Bellot-Gurlet, L.; Bourdonnec, F.-X.L.; Poupeau, G.; Dubernet, S. Raman Micro-Spectroscopy of Western Mediterranean Obsidian Glass: One Step towards Provenance Studies? *J. Raman Spectrosc.* **2004**, *35*, 671–677. [CrossRef]
25. Moutsiou, T. A Compositional Study (PXRF) of Early Holocene Obsidian Assemblages from Cyprus, Eastern Mediterranean. *Open Archaeol.* **2019**, *5*, 155–166. [CrossRef]
26. Tykot, R.H. A Decade of Portable (Hand-Held) X-ray Fluorescence Spectrometer Analysis of Obsidian in the Mediterranean: Many Advantages and Few Limitations. *MRS Adv.* **2017**, *2*, 1769–1784. [CrossRef]
27. Martinelli, M.C.; Tykot, R.H.; Vianello, A. Lipari (Aeolian Islands) Obsidian in the Late Neolithic, Artifacts, Supply and Function. *Open Archaeol.* **2019**, *5*, 46–64. [CrossRef]
28. Tykot, R.H. Geological Sources of Obsidian on Lipari and Artifact Production and Distribution in the Neolithic and Bronze Age Central Mediterranean. *Open Archaeol.* **2019**, *5*, 83–105. [CrossRef]
29. Tykot, R.H. Characterization of the Monte Arci (Sardinia) Obsidian Sources. *J. Archaeol. Sci.* **1997**, *24*, 467–479. [CrossRef]
30. Tykot, R.H. Non-Destructive PXRF on Prehistoric Obsidian Artifacts from the Central Mediterranean. *Appl. Sci.* **2021**, *11*, 7459. [CrossRef]
31. Freund, K.P.; Tykot, R.H.; Vianello, A. Blade Production and the Consumption of Obsidian in Stentinello Period Neolithic Sicily. *Comptes Rendus Palevol.* **2015**, *14*, 207–217. [CrossRef]
32. De Francesco, A.; Bocci, M.; Crisci, G.M.; Francaviglia, V. Obsidian Provenance at Several Italian and Corsican Archaeological Sites Using the Nondestructive X-ray Fluorescence Method. In *Obsidian and Ancient Manufactured Glasses*; Liritzis, I., Stevenson, C.M., Eds.; University of New Mexico Press: Albuquerque, NM, USA, 2012; pp. 115–129.
33. Conrey, R.M.; Goodman-Elgar, M.; Bettencourt, N.; Seyfarth, A.; Van Hoose, A.; Wolff, J.A. Calibration of a Portable X-ray Fluorescence Spectrometer in the Analysis of Archaeological Samples Using Influence Coefficients. *Geochem. Explor. Environ. Anal.* **2014**, *14*, 291–301. [CrossRef]
34. Agha-Aligol, D.; Lamehi-Rachti, M.; Oliaiy, P.; Shokouhi, F.; Farahani, M.F.; Moradi, M.; Jalali, F.F. Characterization of Iranian Obsidian Artifacts by PIXE and Multivariate Statistical Analysis. *Geoarchaeology* **2015**, *30*, 261–270. [CrossRef]
35. Prokeš, L.; Vašinová Galiová, M.; Hušková, S.; Vaculovič, T.; Hrdlička, A.; Mason, A.Z.; Neff, H.; Přichystal, A.; Kanický, V. Laser Microsampling and Multivariate Methods in Provenance Studies of Obsidian Artefacts. *Chem. Pap.* **2015**, *69*, 761–778. [CrossRef]
36. Bonizzoni, L.; Galli, A.; Milazzo, M. Direct Evaluation of Self-Absorption Effects in Dark Matrices by Compton Scattering Measurements. *X-ray Spectrom.* **2000**, *29*, 443–448. [CrossRef]

37. Bonizzoni, L.; Galli, A.; Spinolo, G.; Palanza, V. EDXRF Quantitative Analysis of Chromophore Chemical Elements in Corundum Samples. *Anal. Bioanal. Chem.* **2009**, *395*, 2021–2027. [CrossRef]
38. Acquafredda, P. XRF Technique. *Phys. Sci. Rev.* **2019**, *4*, 1–20. [CrossRef]
39. Van Espen, P.; Janssens, K.; Swenters, I. *IAEA Computer Manual Series No. 21 (IAEA/CMS/21/CD)*; IAEA: Vienna, Austria, 2009.
40. Hughes, R.E. The Coso Volcanic Field Reexamined: Implications for Obsidian Sourcing and Hydration Dating Research. *Geoarchaeology* **1988**, *3*, 253–265. [CrossRef]
41. Tykot, R.H. Inter-Instrumental Calibration and Data Comparison for XRF Analysis of Obsidian and Other Archaeological Materials. In Proceedings of the 43rd International Symposium on Archaeometry, Lisbon, Portugal, 16–20 May 2022.
42. Saleh, M.; Bonizzoni, L.; Orsilli, J.; Samela, S.; Gargano, M.; Gallo, S.; Galli, A. Application of Statistical Analyses for Lapis Lazuli Stone Provenance Determination by XRL and XRF. *Microchem. J.* **2020**, *154*, 104655. [CrossRef]
43. Durrani, S.A.; Khan, H.A.; Taj, M.; Renfrew, C. Obsidian Source Identification by Fission Track Analysis. *Nature* **1971**, *233*, 242–245. [CrossRef]
44. Chataigner, C.; Badalian, R.; Bigazzi, G.; Cauvin, M.-C.; Jrbashian, R.; Karapetian, S.G.; Norelli, P.; Oddone, M.; Poidevin, J.-L. Provenance Studies of Obsidian Artefacts from Armenian Archaeological Sites Using the Fission-Track Dating Method. *J. Non-Cryst. Solids* **2003**, *323*, 167–171. [CrossRef]
45. Bellot-Gurlet, L.; Bigazzi, G.; Dorighel, O.; Oddone, M.; Poupeau, G.; Yegingil, Z. The Fission-Track Analysis: An Alternative Technique for Provenance Studies of Prehistoric Obsidian Artefacts. *Radiat. Meas.* **1999**, *31*, 639–644. [CrossRef]
46. Bigazzi, G.; Ercan, T.; Oddone, M.; Özdoğan, M.; Yeğingil, Z. Application of Fission Track Dating to Archaeometry: Provenance Studies of Prehistoric Obsidian Artifacts. *Nucl. Tracks Radiat. Meas.* **1993**, *22*, 757–762. [CrossRef]
47. Ruschioni, G.; Micheletti, F.; Bonizzoni, L.; Orsilli, J.; Galli, A. FUXYA2020: A Low-Cost Homemade Portable EDXRF Spectrometer for Cultural Heritage Applications. *Appl. Sci.* **2022**, *12*, 1006. [CrossRef]
48. Bonizzoni, L.; Galli, A.; Gondola, M.; Martini, M. Comparison between XRF, TXRF, and PXRF Analyses for Provenance Classification of Archaeological Bricks. *X-ray Spectrom.* **2013**, *42*, 262–267. [CrossRef]
49. Micheletti, F.; Orsilli, J.; Melada, J.; Gargano, M.; Ludwig, N.; Bonizzoni, L. The Role of IRT in the Archaeometric Study of Ancient Glass through XRF and FORS. *Microchem. J.* **2020**, *153*, 104388. [CrossRef]
50. Baxter, M.J. A Review of Supervised and Unsupervised Pattern Recognition in Archaeometry. *Archaeometry* **2006**, *48*, 671–694. [CrossRef]
51. R Core Team. *R: A Language and Environment for Statistical Computing*; R Foundation for Statistical Computing: Vienna, Austria, 2021. Available online: https://www.r-project.org/ (accessed on 1 February 2023).
52. Fernández-Ruiz, R.; García-Heras, M. Study of Archaeological Ceramics by Total-Reflection X-ray Fluorescence Spectrometry: Semi-Quantitative Approach. *Spectrochim. Acta Part B At. Spectrosc.* **2007**, *62*, 1123–1129. [CrossRef]
53. Idjouadiene, L.; Mostefaoui, T.A.; Djermoune, H.; Ziat, F.; Bonizzoni, L. XRF Analysis of Ancient Numidian Coins: A Comparison between Different Kingdoms. *Eur. Phys. J. Plus* **2021**, *136*, 512. [CrossRef]